J Fluoresc (2013) 23:671–679
DOI 10.1007/s10895-013-1174-1

ORIGINAL PAPER

The Effect of Translational Motion on FLIM Measurements-Single Particle Phasor-FLIM

Alireza Lajevardipour · Andrew H. A. Clayton

Received: 9 December 2012 / Accepted: 24 February 2013 / Published online: 8 March 2013

Abstract Fluorescence lifetime imaging microscopy or FLIM provides a versatile tool for spatially-mapping macromolecular interactions and environments through pixel-by-pixel resolution of the excited-state lifetime. In conventional frequency-domain FLIM the phase and modulation of the detected fluorescence are determined by the photophysics of the fluorophore only. However, translational motion on the timescale of FLIM acquisition can significantly perturb apparent phase and modulation values owing to intensity fluctuations and phase decoherence. Using the phasor plot we outline a simple analytic theory, numerical simulations and measurements on fluorescent beads (ex 470 nm, em 520 nm). Fluctuations due to particle motions result in an increase in the number and spread of phasors, an effect we refer to as phasor broadening. The approach paves the way for the measurement of lifetimes and translational motion from one experiment.

Keywords FLIM · Phase decoherence · Fluorescence fluctuation spectroscopy · Fluorescence lifetime imaging microscopy · Diffusion

Introduction

FLIM or fluorescence lifetime imaging microscopy [1] is traditionally a useful tool for spatially-mapping fluorescence lifetimes and interactions (through FRET [2]. In the vast majority of cases, lateral motions are either frozen (e.g. fixed cells), averaged on the timescale of the measurement (e.g. solutions), or observed but considered as an artefact [3]. Here determine the influence of lateral motions of particles upon FLIM experiments. The basic idea is illustrated in Fig. 1. In frequency-domain analysis of FLIM the intrinsic time-resolved fluorescence is characterized by the properties of a sinusoidal function (phase and modulation values) at a given modulation frequency (frequency-domain instrumentation) or laser repetition frequency (time-domain instrumentation). In FLIM with moving particles, occupancy fluctuations of fluorescent species cause a phase decoherence of this normal sinusoidal intensity profile resulting in a deviation in the phase and modulation values. This perturbation can be visualized most conveniently in phasor space [4–7] as a blooming or spreading of phasors. We first demonstrate using a simple "back of the envelope" analytic theory how extreme particle fluctuations can perturb phasor positions for a single particle. We then use numerical simulations with Gaussian convoluted particle to demonstrate motion-related phasor broadening. Finally, we simulate a collection of Brownian-like moving particles and it is explicitly shown how the variance in the phasor plot is related to the extent of particle motion. The effect of noise is examined and an experimental demonstration of the phasor broadening effect is provided with fluorescent beads.

The analysis and results presented on the one hand reveal how lateral motions can influence lifetime measurements. When these motions are significant enough to cause broadening of apparent lifetime distributions then information about these motions can be extracted. On the other hand the analysis provides a complementary way of measuring intensity fluctuations and average lifetimes in the one experiment.

A. Lajevardipour · A. H. A. Clayton (✉)
Centre for Micro-photonics, Faculty of Engineering and Industrial Sciences, Swinburne University of Technology, John Street, PO Box 218, Hawthorn, Victoria 3122, Australia
e-mail: aclayton@swin.edu.au

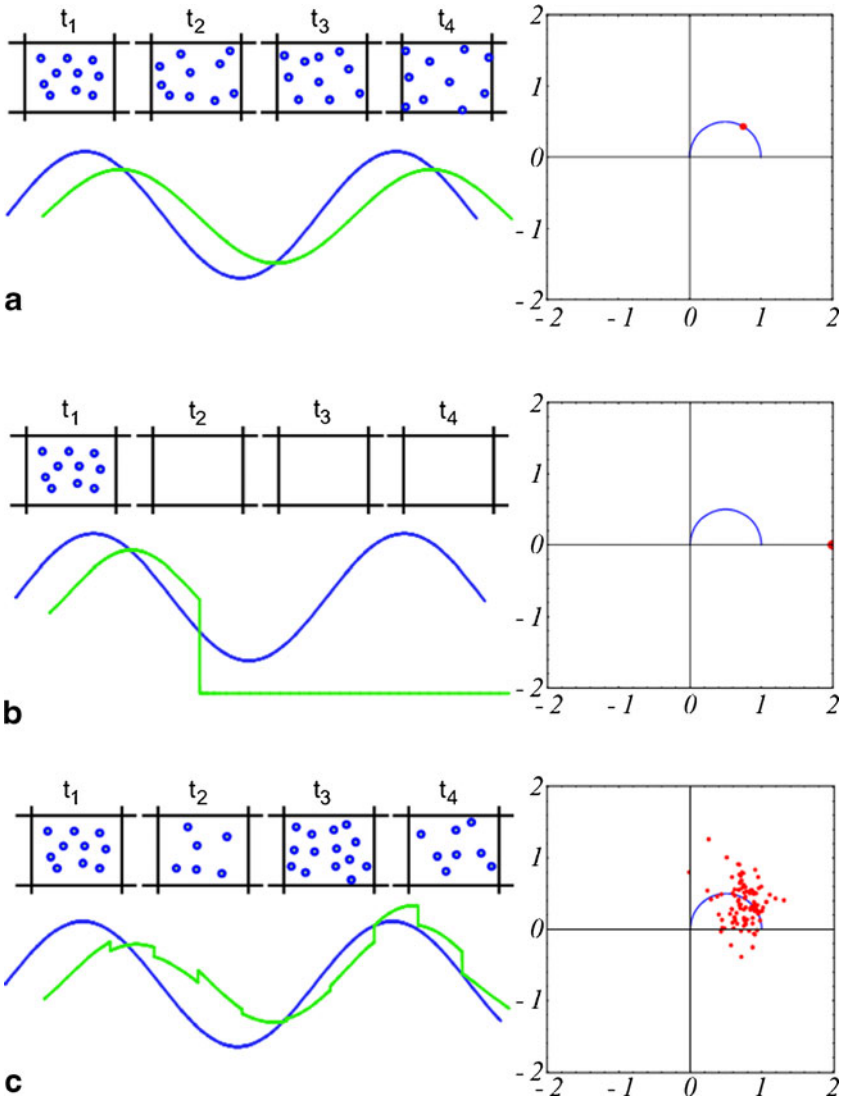

Fig. 1 Qualitative concept of FLIM with moving particles. *Left column*; **a** Projected fluorescent particles in a CCD pixel at different times with no change in number of particles. *Blue line*; modulated excitation, *Green line*; detected emission (*sine wave*). **b** The CCD pixel at different times with extreme change in particle number. *Blue line*; modulated excitation, *Green line*; detected emission. Note distorted sinewave detected due to large particle number fluctuation. **c** The CCD pixel at different times with moderate change in particle number. *Blue line*; modulated excitation, *Green line*; detected emission. Note slightly distorted sine-wave detected due to moderate particle number fluctuation. *Right column*; Phasor plots for FLIM depend on particle occupancy. **a** Phasor plot for frozen single particle (no movement). **b** Phasor plot for occupancy sequence (1,0,0,0), and **c** fluctuations about an average occupancy leading to phasor plot broadening

Materials and Methods

Numerical Simulations

The complete numerical simulation can be divided in the two sub-simulations; simulation of beads movement and simulation of FLIM experiment.

To simulate Brownian motion, a FORTRAN code was developed to solve the Langevin equation with velocity Verlet algorithm (M. P. Allen and D. J. Tildesley. 1989). Simulated particles were moved stochastically on the surface of an image grid with size of 1392×1040 pixels (size of a regular CCD) but 2 by 2 binning where each pixel has a binned size of 12.9 μm×12.9 μm. To place initial position, particles were distributed randomly on the image grid with random initial velocities.

We simulated three different ensembles, 100 point-like particles, a single Gaussian bead with size 21 by 21 pixels, and two Gaussian beads (each with size 21 by 21 pixels). We took some snapshot (e.g. 10 images) at equal intervals among whole duration of simulation as we need them for FLIM calculation.

To ensure the simulations conformed to Brownian behavior, and to provide a measure of extent of motion, we computed the mean square displacement (MSD) as follows:

$$\mathrm{MSD} = \left\langle \frac{1}{N} \sum_{l=1}^{N} \left(x_l(k) - x_l(0)\right)^2 + \left(y_l(k) - y_l(0)\right)^2 \right\rangle \tag{1}$$

Where x, y are spatial coordinates of particle l in image number of k. N represents the total number of particles. As expected for normal diffusive motion, the MSD values scaled linearly with time.

To simulate the FLIM experiment, we assumed sinusoidal behavior of the detected intensity as a function of phase delay between fluorescence and detector. Moreover, for simplicity we assumed single exponential decay of the fluorescence with

fixed phase (φ) and modulation ($m = \cos\varphi$). The total intensity as a function of image number and pixel location is then given by the equation,

$$I_{i,j}(k) = n_{i,j}(k)\left[1 + \cos\varphi * \cos\left(\frac{2\pi}{K}k - \varphi\right)\right] \quad (2)$$

Where i and j are pixel indices and $n_{i,j}(k)$ is the number of particles in a pixel element (e.g. 0, 1, 2, …) in point-like particles ensemble and is the element of Gaussian matrix for single Gaussian ensemble, both at image number k, where the total number of captured images (K) is 10 here. As one can infer the image number (k) plays the role of time in our simulation. To extract the phase and modulation of the detected signal we used classical Fourier analysis techniques as described elsewhere such as [1, 8–10]. By inspection of Eq. (2) it is clear that if $n_{i,j}(k)$ is a constant in a particular pixel for all k then the phase of the detected signal will be φ and the modulation will be $m = cos\varphi$. We put $\varphi = \pi/6$ in our simulation then as shown in Fig. 1a, the simple output is ($m\ cos\varphi$, $m\ sin\varphi$)=(0.75, 0.43). However, if $n_{i,j}(k)$ is not constant for all ks, i.e. particles move in or out of the pixel, then the detected phase and modulation will not be equal to φ and $cos\varphi$, respectively.

In the latter case the phasor plots contain several points related to different detected phase and modulation. The mean value of the phasor ($\langle m\cos\varphi\rangle$, $\langle m\sin\varphi\rangle$) was determined by;

$$\langle m\cos\varphi\rangle = \tfrac{1}{n}\sum(m\cos\varphi)_q \quad ; \quad \langle m\sin\varphi\rangle = \tfrac{1}{n}\sum(m\sin\varphi)q \quad (3)$$

Where $\sum$ represents the sum of n data points (q).

The variance was computed using the equation

$$Var = \sqrt{\langle R^2\rangle - \langle R\rangle^2} \quad (4)$$

Where R is the distance between the mean phasor value and a given point on the phasor plot, R^2 is the square of the distance, $\langle R^2\rangle$ is the average squared-distance for all points and $\langle R\rangle^2$ is the average distance for all points-squared.

To stimulate noise into our simulation, we exploit multiplication of random numbers to detected intensity that could have an effect only on specific percentage of detected intensity of a bead as shown in Eq. 5.

$$I_{i,j}(k) = n_{i,j}(k)\left[1 + \cos\varphi * \cos\left(\frac{2\pi}{10}k - \varphi\right)\right] \times (1 - p + p * \xi_n) \quad (5)$$

Where p is fraction of detected intensity that fluctuates, ξ_n is a random number in the range of 0 to1 for each $n_{i,j}(k)$.

In simulation of particle motions, we can adjust parameters of Langevin equation to produce different ensembles with various MSDs. Then we use these ensembles in simulation of FLIM experiment. At the end, we relate variance in phasor plot caused by movement of beads to MSD of movements.

Based on the nature of random walk, ensembles with the same MSD may produce slightly different variance on phasor plot depend on history of movements (e.g. initial random position of beads and probable passing border of pixel). It can cause an error in relating diffusion coefficient to variance so that we needed to take this variance error into account.

Fluorescence Lifetime Imaging Microscopy

To confirm our simulation results experimentally, we performed FLIM measurements on moving fluorescent beads. Coverslips were washed with methanol and surfaces were then treated with 1× phosphate buffered saline (PBS) solutions plus 5 % bovine serum albumin (BSA). This protein treatment pacified the surface and reduced the likelihood of bead adsorption during experimentation.

Ten uL of 2.5 micron fluorescent beads (100 % intensity, In-Speck, Invitrogen) in 200 uL water and 1× PBS plus 5 % BSA was placed between two coverslips. A Nikon microscope with Lambert instruments LIFA (The Netherlands) FLIM attachment was employed to measure FLIM images of the moving beads [11] for details). The beads were excited with sinusoidally- modulated (40 MHz) 470 nm light focused through a 100×, 1.4NA oil objective and the emission was observed through a 515LP filter. Ten phase steps were recorded at four different exposure times (2 ms, 4 ms, 5 ms and 10 ms) using software provided by the manufacturer. Rhodamine 6 G in distilled water (lifetime=4.1 ns) was used as a reference [3]. Lambert LI-FLIM software was used for all analysis of experimental data.

The phasor plots were exported using the Lambert LI-FLIM software. The mean value of the phasor and its variance were computed using Eqs. (3) and (4), respectively.

The lifetimes of the beads were τ_p=4 ns and τ_m=4 ns (determined from an immobilized sample).

Results and Discussion

Frequency-Domain FLIM at Steady-State

FLIM measures the lifetime of fluorescence on a pixel-by-pixel basis [3, 10]. In the frequency-domain method the intensity at a single pixel follows a sinusoidal profile as a function of phase delay (homo-dyne) or time (heterodyne detection). Analysis of the function, using Fourier techniques delivers the phase and modulation of the detected signal.

Let us first consider conventional FLIM where the concentration of species is assumed to be either fixed or at steady-state during acquisition. For simplicity we consider a simple 4-phase ($K=4$ in Eq. 2) homodyne experiment as this is analytically tractable. Beginning with the detected signal $I_k(\varphi)$ as a function of the image number k we write;

$$I_k(\varphi) = DC + AC * \cos\left(\frac{2\pi}{4}k - \varphi\right) \tag{6}$$

Where DC is unmodulated signal component, AC is the amplitude of the modulation signal component, and φ is a phase difference between the excitation and emission. We can measure the intensities at detector phase positions 0, $\pi/2$, π, $3\pi/2$ (corresponding to k=0, 1, 2, 3). Using Fourier techniques, the phase and modulation of the detected signal can be determined from the cosine and sine transforms. Applying this techniques to the Eq. (6) for k=0, 1, 2 and 3, the components of the phasor can be represented in terms of intensities and are given by the equations;

$$\begin{aligned} m\cos\varphi &= 2(I_0 - I_2)/(I_0 + I_1 + I_2 + I_3) \\ m\sin\varphi &= 2(I_1 - I_3)/(I_0 + I_1 + I_2 + I_3) \end{aligned} \tag{7}$$

Note that we do not explicitly mention the modulation frequency in these equations since in the homodyne method one records essentially a steady-state signal at each phase setting (k) on the detector. The modulation frequency appears intrinsically in the relationship between the phase, modulation and the fluorescence lifetime (for example, for a single component lifetime system, $tan\varphi = \omega\tau$, where τ is lifetime ω is the modulation frequency and φ is the phase.

Frequency-Domain FLIM Including Single Particle Fluctuations

Let us now consider the effect of particle fluctuations on the phase and modulation values or more precisely the phasor components. We will consider the most rudimentary type of particle fluctuation- the particle is either inside the observation volume at a given time and has an intensity value $I(\varphi)$ (see Eq. 2) at the observed detector phase position or is not inside the observation volume at that time (or phase position) and has an intensity value of zero. Table 1 lists the possible binary combinations of particle occupancies and corresponding modulation and phase values (represented by the phasor components) for the 4-phase example using Eq. 6. It is clear that if the particle is present in the observation volume during all phase recordings then the phase and modulation measured will be the true phase and modulation expected. However, if the particle occupancy is not constant during all four phase recordings then the phase and modulation values no longer represent the true lifetime of the fluorophore. A very convenient depiction of these effects is with the polar plot (phasor plot or AB-plot) which is a plot of $x = m\cos\varphi$ as a function of $y = m\sin\varphi$, see Fig. 1. For the non-fluctuation case, the fluorescence appears as a single point on the phasor diagram, as expected. (Parenthetically we recall that for all time-resolved fluorescence decays, even of multicomponent fluorescence with non-negative amplitudes the phasor positions are located within the semi-circle [12].) However it is seen that inclusion of fluctuations can cause an expansion in the possible values on the phasor plot. The maximal excursion appears to occur at values of (2,0), (0,2), (0,−2), (−2,0) (Table 1) where the

Table 1 Computed phasor components as a function of particle occupancy for an idealized four-phase FLIM experiment

Particle occupancy	Intensity	x	y
1,1,1,1	I_0,I_1,I_2,I_3	$m\,cos\varphi$	$m\,sin\varphi$
0,1,1,1	0,I_1,I_2,I_3	$(2\,m\,cos\varphi - 2)/(3 - m\,cos\varphi)$	$(2m\,sin\varphi)/(3 - m\,cos\varphi)$
1,0,1,1	I_0,0,I_2,I_3	$(2m\,cos\varphi)/(3 - m\,sin\varphi)$	$(2m\,sin\varphi - 2)/(3 - m\,sin\varphi)$
1,1,0,1	I_0,I_1,0,I_3	$(2 + 2m\,cos\varphi)/(3 + m\,cos\varphi)$	$(2m\,sin\varphi)/(3 + m\,cos\varphi)$
1,1,1,0	I_0,I_1,I_2,0	$(2m\,cos\varphi)/(3 + m\,sin\varphi)$	$(2 + 2m\,sin\varphi)/(3 + m\,sin\varphi)$
0,0,1,1	0,0,I_2,I_3	$(2m\,cos\varphi - 2)/(2 - m\,cos\varphi - msin\varphi)$	$(2m\,sin\varphi - 2)/(2 - m\,cos\varphi - msin\varphi)$
1,0,1,0	I_0,0,I_2,0	$2\,m\,cos\varphi$	0
1,1,0,0	I_0,I_1,0,0	$(2 + 2m\,cos\varphi)/(2 + m\,cos\varphi + msin\varphi)$	$(2 + 2m\,sin\varphi)/(2 + m\,cos\varphi + m\,sin\varphi)$
1,0,0,1	I_0,0,0,I_3	$(2 + 2m\,cos\varphi)/(2 + m\,cos\varphi - m\,sin\varphi)$	$(2 - 2m\,sin\varphi)/(2 + m\,cos\varphi - m\,sin\varphi)$
0,1,1,0	0,I_1,I_2,0	$(2m\,cos\varphi - 2)/(2 - m\,cos\varphi + msin\varphi)$	$(2 + 2m\,sin\varphi)/(2 - m\,cos\varphi + m\,sin\varphi)$
0,1,0,1	0,I_1,0,I_3	0	$2\,m\,sin\varphi$
1,0,0,0	I_0,0,0,0	2	0
0,1,0,0	0,I_1,0,0	0	2
0,0,1,0	0,0,I_2,0	−2	0
0,0,0,1	0,0,0,I_3	0	−2

particle appears only once during 4-phase acquisitions. Simulations with other numbers of phase steps indicate that the magnitude of the phasors during motion also do not exceed 2 (see also example for ten phase steps). This is not a simulation effect but rather comes from the nature of the equations. Note that the actual phasor position provides a unique 2D map of the particle occupancy sequence (or more precisely the intensity sequence), (Table 1). We only consider single particle occupancies here at this point but investigate other types of occupancies later using simulations.

Now consider a collection of observation volumes in an imaging experiment. In an imaging arrangement with an array detector such as a CCD camera, each volume element can be considered a pixel or set of pixels. If we consider very fast movement of a single particle from one region to the next to the next, etc will produce a (1,0,0,0) occupancy sequence in one region, a (0,1,0,0) occupancy in the next, (0,0,1,0) and so on. The resulting single phasor for one stationary particle (no movement) will become 4 phasors for a rapidly moving particle. We refer to the change in a single phasor to multiple phasors as phasor broadening.

Phasor-FLIM During Motion of a Single Large Gaussian Particle

The aforementioned example is somewhat idealized because the particle fluctuations are considered as binary events. We simulated a FLIM experiment with a moving Gaussian particle of a size that occupies many area elements (21 by 21 pixels). The phasor of the particle without movement is shown in Fig. 2a. The calculated phasor plot with increasing extents of stochastic particle movement (over 10 phase steps) is shown in Fig. 2b–f for comparison. As the extent of motion is increased the number of points outside the semi-circle on the phasor plot increases. At maximal movement simulated, the phasor diagram contains 10 points located at a radius of 2 on the phasor plot. This is analogous to the 4-phase example.

Phasor-FLIM for an Ensemble of Particle Motions

For random (essentially Brownian) motion a particle ensemble will undergo different types of occupancy fluctuations (e.g. 0, 1, 2, 0, 3 etc.). It is useful to simulate these effects and to calculate the resulting phasor diagram. For this purpose we simulated the effects of having a large fixed number of Brownian particles of point-like size and determined the influence of extent of motion on the phasor plot (see Fig. 3). Figure 4 plots the mean-squared displacement as a function of time from the simulations. Note the linearity of the MSD versus time plot is consistent with random motion. Figure 3 displays corresponding phasor plots for different extents of motion. Qualitatively it is clear that with no motion all particles have identical phasor position while with some random motion some of the particles have phasor positions that are significantly perturbed with respect to the expected position. Increasing the extent of motion increases the number and excursion of points away from the expected phasor position. Plotting the variance of data points in the phasor plot and MSD, both as a function of time (Fig. 4), it is inferable that the variance is directly correlated with MSD.

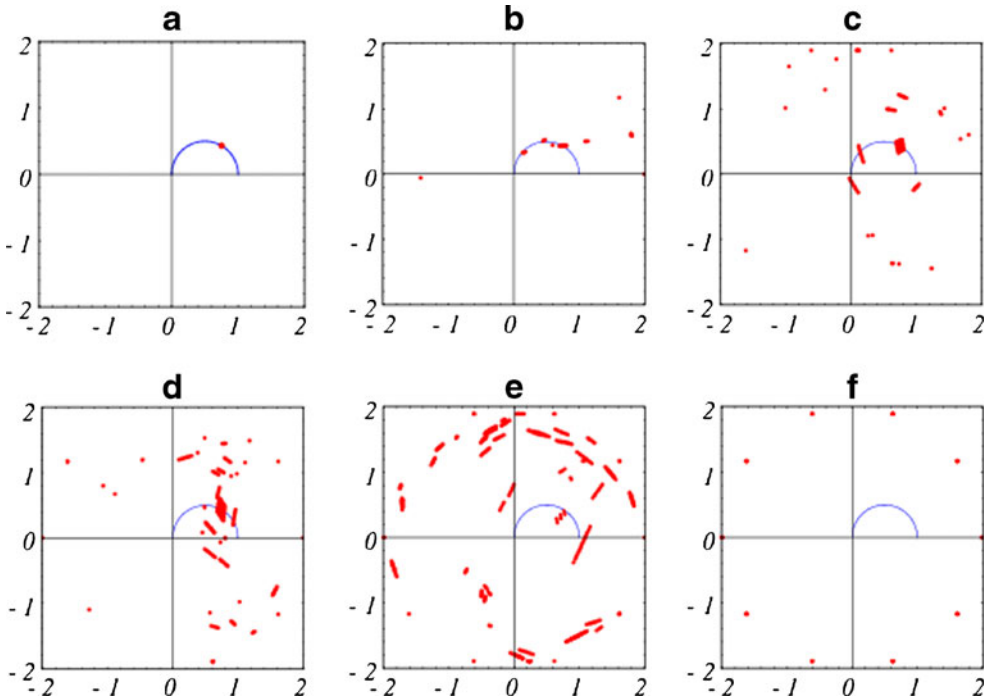

Fig. 2 Phasor plots for FLIM during movement of a single particle. Simulation of the motion of single Gaussian particle projected to 21 by 21 CCD pixels each 6.45 μm by 6.45 μm. **a** Phasor plot for Gaussian particle with no motion **b** Phasor plot for small amount of Brownian motion where projected MSD on CCD is $5.63\times10^{-5} mm^2$ at the 10th image. In this case the variance in phasor plot is 0.59 **c** Phasor plot for larger extent of motion (with projected MSD on CCD of $1.69\times10^{-4} mm^2$ at the 10th image). The variance in phasor plot is 0.76 **d** (MSD, Variance) $=(2.72\times10^{-3} mm^2, 1.07)$ **e** (MSD, Variance)$=(3.29\times10^{-2} mm^2, 1.82)$ **f** (MSD, Variance) =(2.28,2)

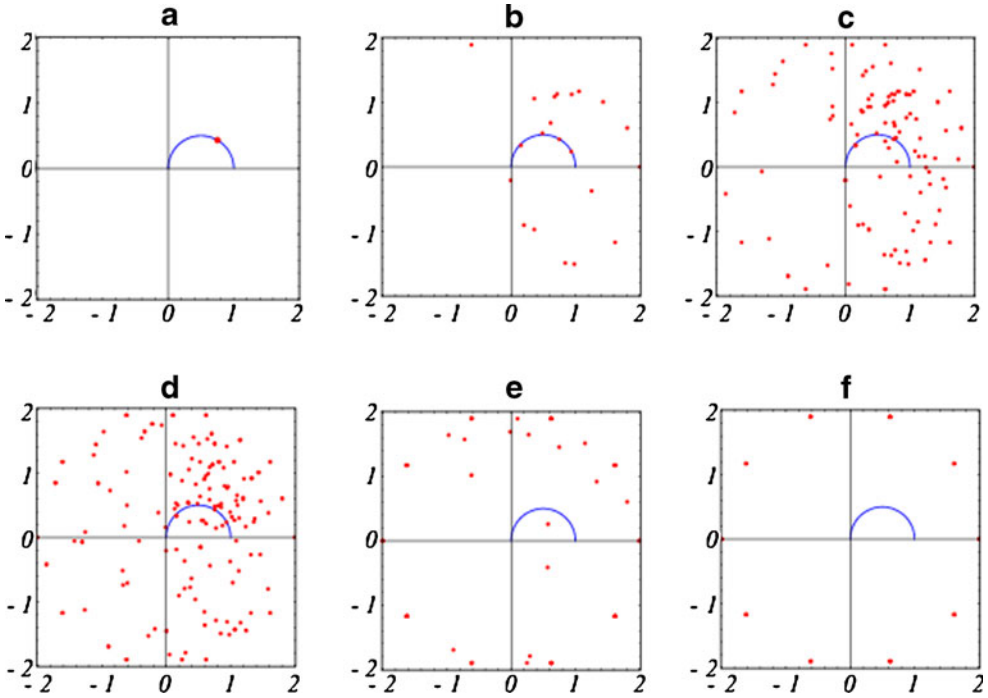

Fig. 3 FLIM simulation of collection of point particle motions. Six different ensembles of 100 beads with stochastic movement were used in the simulation. **a** Phasor plot of 100 beads with no motion. **b** Phasor plot with 100 beads with some Brownian motion with $MSD=9.9\times10^{-7} mm^2$ (variance in phasor plot is 0.55) **c** Phasor plot with increased particle motion (MSD, Variance)=$(1.43\times10^{-5}$ mm^2,1.37) **d** Phasor plot. (MSD,Variance)=$(5.72\times10^{-5}$ mm^2,1.61) **e** Phasor plot (MSD, Variance)=$(1.36\times10^{-2}$ mm^2,1.99) **f** Phasor plot (MSD, Variance)=$(7.4\times10^{-1} mm^2$,2)

The blooming of the phasor plot grows with increasing particle movement up to a certain point. At this point the phasor positions have reached their extreme positions and the variance is independent of extent of motion afterwards.

Effect of Noise and Motion on Phasor Plots

In real FLIM images, even of homogenous solutions, the phasor plots have some finite width due to noise in the system (for an excellent discussion of noise refer to [13]). As an indication the measured phase and modulation lifetimes have typical standard deviations of about 0.1 ns under optimal measurement conditions. Clearly, even noisier FLIM images result when photon noise increases in the case of weak emission or for rapid FLIM acquisition. We have simulated the effect of adding noise on the width of resulting phasor plots for no particle movement and for varying degrees of particle motion. As expected, adding noise increases the width of phasor plots even without any particle motion (see Fig. 5). However noise has a less dramatic effect on the total phasor broadening for particles undergoing motion. This is illustrated in the inset of Fig. 5a. For example when the variance in the phasor plot due to particle motion is large, adding noise does not appreciably increase the total variance. The motion-effect on the variance is much larger than the noise effect.

In practice photon noise will be always present in the detector and this noise will depend on the features of the

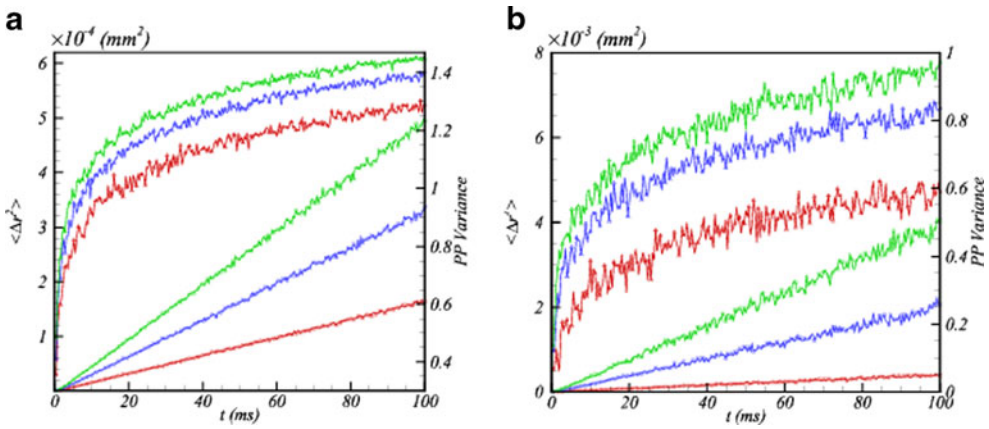

Fig. 4 **a** Plot of the variance in phasor plot as a function of time compared with the MSD as a function of time for three different diffusion coefficients where *square symbol* represents MSD and *triangle* represents variance. *Red* represents particles diffusing with $D = 4.95 \times 10^{-4}\ mm^2 s^{-1}$, *Blue* represents simulation for particles with diffusion constant $D = 1.0 \times 10^{-3}\ mm^2 s^{-1}$ and *Green* represents $D = 1.51 \times 10^{-3}\ mm^2 s^{-1}$. The plot was generated from simulation of 100 point-like beads. **b** Same plot as **a** but for two single Gaussian particles

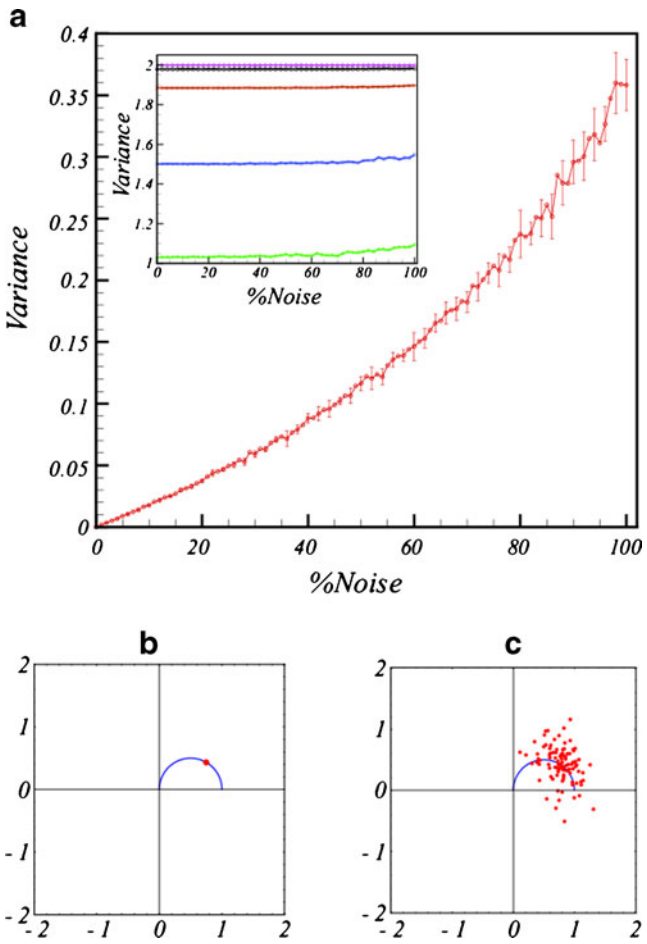

Fig. 5 Effect of noise on phasor plots for FLIM. **a** Plot of the variance in phasor plot as a function of noise (*red line*, main figure) for static beads. Inset; Plot of variance versus noise for different extents of particle motion where *green*, *blue*, *brown*, *black* and *pink lines* represent ensembles used with different MSDs. **b** Phasor plot of static beads without noise. **c** Static beads with 100 % noise

system as well as the exposure time. In general increasing the exposure time will decrease the photon noise due to signal integration. If the exposure time is faster than the transit time of a particle through the observation volume then increasing the exposure time will increase the chance of motion and increase the variance in the phasor plot. On the other hand if the exposure time is already too long-much longer than the transit time for particle movement through the observation volume-then increasing the exposure time will simply increase the averaging of signals. Therefore in practice any increase in the variance of the phasor plot with increased exposure time must be due to motion effects and not noise.

Fluorescent Bead Motions Examined Using FLIM

To provide a concrete experimental example, we measured frequency-domain FLIM images of 2.5 micron diameter fluorescent beads. We used a commercially-available FLIM set-up under wide-field excitation/detection conditions

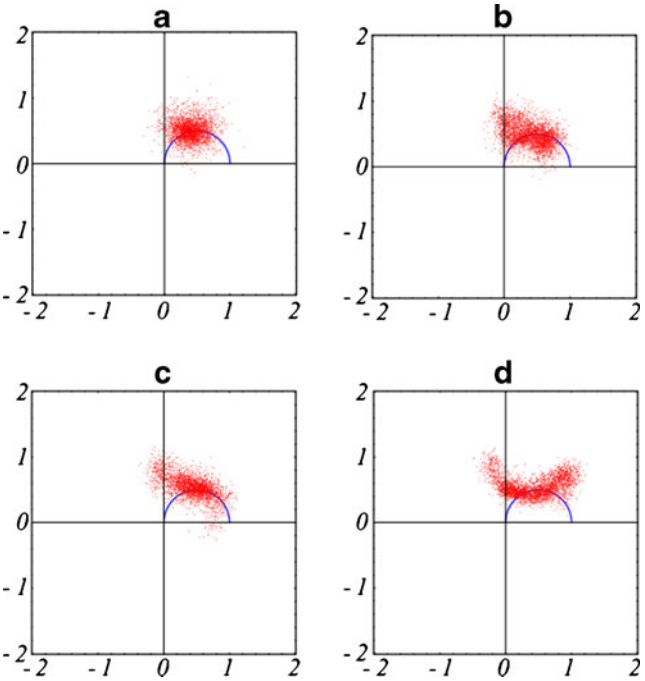

Fig. 6 Experimental FLIM measurement of fluorescent beads. **a** Phasor plor for an exposure time of 2 ms per image (phasor plot variance is 0.2438) **b** Phasor plot (exposure time of 4 ms per image and phasor variance of 0.3104) **c** Phasor plot (exposure time of 5 ms per image and phasor variance is 0.3256) **d** Phasor plot (exposure time of 10 ms per image and phasor variance of 0.3968)

using ten phase steps. To vary the probability of motion during acquisition we varied the exposure time per phase image. Figure 6 displays phasor plots of the fluorescent beads as a function of exposure time. Figure 6a, b, c and d respectively show that increasing the exposure time increases the broadening in the phasor plots. For fast exposures of 2 ms, the phasor plot resembles a fluorophore in a nearly homogenous environment (Fig. 6a). At the other extreme, (Fig. 6c) a 10 ms second exposure per image causes a significant broadening in the phasor plot. Based on shot noise considerations alone, an increase in exposure time from 2 ms to 10 ms should increase the signal to noise ratio by a factor of $\sqrt{5}$. This would be expected to *decrease* the width of the phasor plot in the absence of particle motion. Therefore the observed increased broadening in the phasor plot cannot be due to increases in signal to noise ratio from increasing the exposure time. A more likely explanation is that the phasor broadening is due to particle motions.

Table 2 collates the measured phasor plot variances from the FLIM experiment as a function of exposure time. To relate the variance to a diffusion coefficient we first prepared 45000 ensembles of two stochastically moving particles with different MSDs. Then we used the ensembles in simulation of FLIM experiment to compute phasor plot variances (see Fig. 7). This plot reveals a non-linear, sigmoidal-like dependence of the phasor plot variance upon the extent of motion. In

Table 2 Motion of fluorescent beads determined by phasor-FLIM. See text for details

Variance (± Std)	Total elapsed time (ms)	MSD ($mm^2 \times 10^{-5}$) (± Std)	D ($mm^2/s \times 10^{-8}$)
0.24375±0.00001	20	2.0±0.8	2.6±1.0
0.3104±0.0001	40	4.0±1.0	2.5±0.8
0.3356±0.0002	50	5.0±1.0	2.3±0.7
0.397±0.002	100	9.0±2.0	2.2±0.6

other words, when the particles do not diffuse significantly from the observation volume, the corresponding variance in the phasor plot is negligible, however when particle diffuse away from the initial positions the resulting intensity fluctuations increase the variance.

We used our fitted curve relating variance to MSD to determine the MSD and diffusion coefficient (D = MSD/(4*time)), as shown in Table 2. By inspection it is clear that the MSD increases with exposure time, as expected. The computed apparent diffusion coefficient, D, ranges from $2.2–2.6 \times 10^{-8}$ mm^2/s and does not appear to vary greatly with exposure time. This suggests that the motion sampled is Brownian-like.

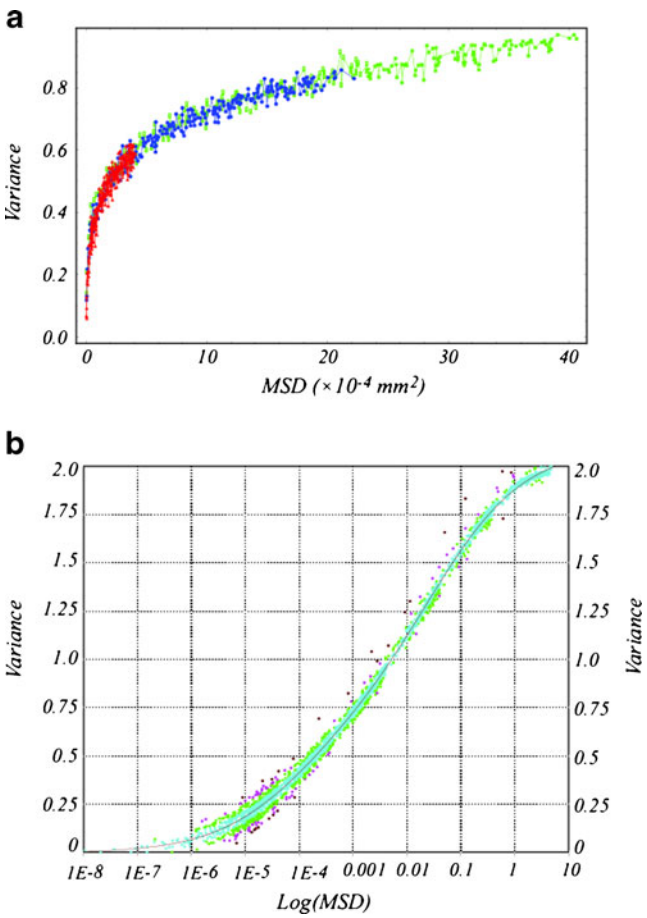

Fig. 7 **a** Plot of the phasor plot variance as a function of MSD from simulations of two moving Gaussian particles. Data was obtained from simulations of three different diffusion coefficients, (*red symbols* (D=1.0×10^{-3} mm^2s^{-1}), *blue symbols* (D=4.65×10^{-3} mm^2s^{-1}), and *green symbols* (D=9.94×10^{-3} mm^2s^{-1}). **b** Plot of the phasor plot variance as a function of the logarithm of MSD. Points are taken from **a** and *solid line* is a fit to the data. Fitted curve function is $y = (c_1 + c_2\sqrt{x} + c_3x)/(1 + c_4\sqrt{x} + c_5x)$ where c_1=−0.0039; c_2=76.1; c_3=1178.0; c_4=106.9; c_5=559.6

There are two different source of error in our derivation of the diffusion coefficient. The first source of error is essentially sampling error. From computer simulations we found that for a given set of conditions there was a variation in the computed MSD and phasor plot variance. This error gives rise to the broad line in Fig. 7b. The second source of error is in the experimental determination of the variance in the phasor plot. We determined this second error experimentally by replicate measurement of the polar plot variance of a rhodamine 6 G solution under different conditions. The errors are given in Table 2.

The experimental result can be compared with theoretical calculation based on the Stokes-Einstein relationship. For beads with radius of 1.25 μm in a solution with viscosity 2.6×10^{-3} Ns m^{-2} (PBS viscosity) and at 19 °C, the diffusion coefficient is calculated to be 6.4×10^{-8} $mm^2 s^{-1}$. This is within an order of magnitude agreement with our experimental result of $2.2–2.6 \times 10^{-8}$ $mm^2 s^{-1}$. This is reasonable agreement given that the apparent diffusion coefficients are derived from ten images of two particles and we have ignored possible influences of BSA and cover-slips on our theoretical estimates.

Scope of the Method

The simulations and experiments were designed to examine the effect of particle motions of fluorescence lifetime imaging microscopy experiments. We deliberately used conditions that would produce the largest effects i.e. single particles and beads. Other conditions (micromolar concentrations) may produce too small a fluctuation to be visible using the phasor approach. This aspect needs to be tested further. One might ask what is new about this approach since methods for determining diffusion coefficients are already well developed. The first difference is that the fluorescence lifetime of the particles can also be determined using this experimental approach. For example, by averaging the data into one pixel the lifetime of the moving particles can be determined. The second difference, is that the position of a point on the phasor plot encodes information about the particle occupancy or intensity fluctuation in that pixel (or group of pixels). For example, if Table 1 we showed that each type of particle occupancy encodes a particular point on the phasor plot.

Conclusions

In the absence of motion a FLIM experiment represents the lifetime of a sample. We have examined the effect of particle motions on FLIM experiments with a particular focus on motions that produce large intensity fluctuations on the time-scale of image acquisition. Motions are conveniently revealed on the phasor diagram. The position of a given pixel on the phasor plot reflects both the intrinsic lifetime of the fluorescent particle and the occupancy history of the particle in that pixel. For population of pixels, the variance of the phasor values is shown to be related to the extent of motion during acquisition. It is shown that the values of the phasor during motion are constrained to lie within a circle with radius 2 in the phasor plot.

Acknowledgments A.L. is a recipient of a Swinburne University Postgraduate Research Award.

Access to the supercomputer facility of Swinburne University is greatly appreciated.

References

1. Chen YC, Spring BQ, Clegg RM (2012) Fluorescence lifetime imaging comes of age how to do it and how to interpret it. Methods Mol Biol 875:1–22
2. Jares-Erijman EA, Jovin TM (2003) FRET imaging. Nat Biotechnol 21(11):1387–1395
3. Hanley QS, Subramaniam V, Arndt-Jovin DJ, Jovin TM (2001) Fluorescence lifetime imaging: multi-point calibration, minimum resolvable differences, and artifact suppression. Cytometry 43(4):248–260
4. Clayton AH, Hanley QS, Verveer PJ (2004) Graphical representation and multicomponent analysis of single-frequency fluorescence lifetime imaging microscopy data. J Microsc 213(Pt 1):1–5
5. Digman MA, Caiolfa VR, Zamai M, Gratton E (2008) The phasor approach to fluorescence lifetime imaging analysis. Biophys J 94(2):L14–L16
6. James NG, Ross JA, Stefl M, Jameson DM (2011) Applications of phasor plots to in vitro protein studies. Anal Biochem 410(1):70–76
7. Redford GI, Clegg RM (2005) Polar plot representation for frequency-domain analysis of fluorescence lifetimes. J Fluoresc 15(5):805–815
8. Noomnarm U, Clegg RM (2009) Fluorescence lifetimes: fundamentals and interpretations. Photosynth Res 101(2–3):181–194
9. Clegg RM, Holub O, Gohlke C (2003) Fluorescence lifetime-resolved imaging: measuring lifetimes in an image. Methods Enzymol 360:509–542
10. Chen YC, Clegg RM (2009) Fluorescence lifetime-resolved imaging. Photosynth Res 102(2–3):143–155
11. Clayton AH, Walker F, Orchard SG, Henderson C, Fuchs D, Rothacker J, Nice EC, Burgess AW (2005) Ligand-induced dimer-tetramer transition during the activation of the cell surface epidermal growth factor receptor-A multidimensional microscopy analysis. J Biol Chem 280(34):30392–30399
12. Gratton E, Jameson DM, Hall RD (1984) Multifrequency phase and modulation fluorometry. Annu Rev Biophys Bioeng 13:105–124
13. Spring BQ, Clegg RM (2009) Image analysis for denoising full-field frequency-domain fluorescence lifetime images. J Microsc 235(2):221–237